Land Degradation and Improvement in China

2. Accounting for soils, terrain and land use change

Z G Bai
Y J Wu
D L Dent
G L Zhang
J A Dijkshoorn
V W P van Engelen
G W J van Lynden

June 2010

LADA

ISRIC **World Soil Information**

FOOD AND AGRICULTURE ORGANIZATION OF THE UNITED NATIONS

This report has been prepared under the conditions laid down in the Letter of Agreement FAO-ISRIC PR 35852.

Preface

The awareness of the importance of our natural resource base as the basic necessity to provide our goods and services is rapidly increasing. With increasing population and increasing wealth the pressure on those resources can be detrimental when not properly managed. Soil provides the solid ground for the production of food and non-food items through agricultural activities and for sustaining world's ecosystems. Preventing its degradation is essential as the availability of fertile soils is limited in the world, constraining expansion of agricultural area. Moreover, soil degradation causes undesirable side effects such as loss of biodiversity, loss of production capacity for agriculture jeopardizing food security, and land slides that sweep away entire villages.

Improper land management in North China causes wind and water erosion that not only decreases local production capacity of the land but also leads to flooding and to dust storms threatening life in cities like Beijing.

China is also concerned about its food provision as the carrying capacity of its land is estimated to be inadequate for the country to be entirely self-sufficient in food. For decision makers to identify where and how to intervene in order to prevent further loss of soil productivity, the severity, location and causes of the degradation should be known.

Modern technologies in remote sensing, ICT, geo-statistics and dynamic simulation methods allow detailed and time-bound analyses of degradation. ISRIC – World Soil Information is engaged in a long term research effort to develop methodologies based on these advanced technologies to assess land degradation. This report presents an approach to identify changes in biomass to be used as an indicator for land degradation. Whereas substantial areas have been identified in China that are subject to biomass decline, the underlying degradation problems and possible causes can only be qualitatively reasoned after consideration of key drivers, such as climate, soil and terrain condition and changes in land use and management. In this report these factors are investigated in relation with the observed changes in biomass.

Further development of a more comprehensive methodology will gradually unfold the character and causes of the observed trends in order to allow better targeting of measures for intervention and decision support.

Dr Ir Prem S Bindraban MBA
Director, ISRIC – World Soil Information

Contents

Figures

Tables

Main Points

1. Land degradation is a global problem. The Global Assessment of Land Degradation and Improvement (GLADA) under the FAO Land Degradation Assessment in Drylands indicates that, over the period of 1981-2003, a quarter of the land surface has been degrading, on top of the historical legacy of degradation (Bai and others 2008a). In China, dry lands have received much attention and reclamation programs have achieved some success but, over the same period, 23 % of the country suffered a decline of climate-adjusted net primary productivity: 24 % of the cropland and 44 % of the forest – not mainly in dry lands but in the high-rainfall areas of South China (Bai and Dent 2009).

2. GLADA analyses long-term trends in biomass productivity using the GIMMS dataset of corrected NDVI 1981-2003. These trends may indicate land degradation or improvement - if false alarms due to climatic variability and land use change can be accounted for. In a preliminary analysis for China (Bai and Dent 2008), climatic variability was taken into account by analysis of rain-use efficiency and energy-use efficiency to separate trends attributed to rainfall variability and increasing temperature. The present analysis updates the GIMMS dataset to 2006 and uses harmonic analysis of the NDVI time series data to remove any residual cloud effects. Soil and terrain effects are then explored using residual trends analysis of soil and terrain condition (SOTER) at 1:1 million scale. Further, for Zhejiang Province, we have extended the analysis to include land use change.

3. The results indicate that one third of the variation in NDVI over the last 26 years is related to long-term rainfall trends but very little to climatic warming. Soil and terrain effects, affecting resilience to land degradation exert a significant influence. Land use change, of itself, leads to changes in biomass that are not necessarily land degradation as ordinarily understood. Unexplained declines in biomass may be related to management practices and other ecosystem disturbances.

Key words: land degradation/improvement, remote sensing, NDVI, rain-use efficiency, net primary productivity, soil and terrain, land use/cover, PR of China

Abbreviations

CGIAR-CSI	Consultative Group on International Agricultural Research, Consortium for Spatial Information
CRU TS	Climate Research Unit, University of East Anglia, Time Series
ENSO	El Niño/Southern Oscillation phenomenon
ENVI	Environment for Visualizing Images – a software for the visualization, analysis, and presentation of all types of digital imagery
EUE	Energy-Use Efficiency
FAO	Food and Agriculture Organization of the United Nations, Rome
FC	Fourier Component
GEF	The Global Environment Facility, Washington DC
GIMMS	The Global Inventory Modelling and Mapping Studies, University of Maryland
GLADA	Global Assessment of Land Degradation and Improvement
GLC	Global Land Cover
GPCC	The Global Precipitation Climatology Centre
HA	Harmonic Analysis
HANTS	Harmonic Analysis of NDVI Time-Series
IDL	Interactive Data Language
ISRIC	ISRIC – World Soil Information
ISRSE	International Symposium on Remote Sensing of Environment
JRC	European Commission Joint Research Centre, Ispra, Italy
LADA	Land Degradation Assessment in Drylands
Landsat TM	Land Resources Satellite Thematic Mapper
LUS	Land Use Systems, FAO
MEA	Millennium Ecosystem Assessment
MOD17A3	MODIS 8-Day Net Primary Productivity dataset
MODIS	Moderate Resolution Imaging Spectroradiometer
NASA	National Aeronautics and Space Administration, USA
NDVI	Normalized Difference Vegetation Index
NPP	Net Primary Productivity
RESTREND	Residual Trend of sum NDVI
RUE	Rain-Use Efficiency
SOTER	Soil and Terrain database
SRTM	Shuttle Radar Topography Mission
UNESCO	The United Nations Educational, Scientific and Cultural Organization
UNCCD	The United Nations Convention to Combat Desertification
UNEP	The United Nations Environment Programme, Nairobi, Kenya
VASClimO	Variability Analyses of Surface Climate Observations

1   Introduction

Land degradation is a chronic and widespread environmental problem (UNEP 2007); it is the focus of the UN Convention to Combat Desertification and a significant issue in the Conventions on Biodiversity and Climate Change. It is one of the environmental stressor on food security of China (McBeath and McBeath 2010). But land degradation is a contentious issue; different parties define it according to their own field of activities, for instance FAO (1979) - 'Land degradation is a process which lowers the … capability of soils to produce'; and the Millennium Ecosystem Assessment (MEA 2005) - 'The reduction in the capacity of land to perform ecosystem goods, functions and services that support society and development'. Most practitioners see it more narrowly in terms of the symptoms observable in the field - such as soil erosion, salinity, nutrient depletion, and the condition of cropland, forest and rangeland.

If we adopt the UNEP (2007) definition 'a long-term loss of ecosystem function and productivity caused by disturbances from which land cannot recover unaided', then land degradation may be measured by long-term change in net primary productivity (NPP) if other factors that may be responsible (climate, soil, terrain and land use) are accounted for. Bai and Dent 2009 used the remotely-sensed normalized difference vegetation index (NDVI) as a proxy for NPP; rainfall effects were accounted for by rain-use efficiency (NDVI per unit of rainfall) and temperature effects by energy-use efficiency (derived from accumulated temperature). This report takes account of soil and terrain differences at national scale that we would expect to influence the resulting patterns of degradation and improvement and, further, considers land use change as a driver of land degradation.

2   Data and methods

2.1   Data

2.1.1 NDVI and net primary productivity

The NDVI data are from the Global Inventory Modeling and Mapping Studies (GIMMS) dataset of AVHRR radiometer measurements by the US National Oceanic and Atmospheric Administration (NOAA) satellites for the period July 1981 to December 2006, corrected for calibration, view geometry, volcanic aerosols and other effects not related to vegetation cover, and generalized as fortnightly images at 8km-spatial resolution (Tucker and others 2004, Pinzon and other 2007). In GIMMS, cloud effects are removed by excluding low values for each 14-day period. We have used the Harmonic Analysis of NDVI Time-Series (HANTS) algorithm (Verhoef and others 1996, Roerink and others 2000, de Wit and Su, 2005) to smooth and reconstruct the NDVI time-series to remove any residual cloud effects

or other outliers (de Jong and others 2009), see Appendix I. Subsequent analysis employs the reconstructed data.

2.1.2 Climatic data

The VASClimO 1.1 dataset comprises the most complete monthly precipitation data for 1951-2000, compiled on the basis of long, quality-controlled station records, 280 in China, gridded at resolution of 0.5° (Beck and others 2005). Monthly rainfall data since January 1981 were extended to 2006 with the GPCC full data re-analysis product (Schneider and others 2008). Rain-use efficiency was calculated as the ratio of annual sum NDVI to annual rainfall. Mean annual temperature values from the CRU TS 3.0 dataset of monthly, station-observed values, also gridded at 0.5° resolution (Mitchell and Jones 2005), were used to calculate the energy-use efficiency as the ratio of annual sum NDVI to annually accumulated temperature; the CRU 3.0 monthly time series cloudiness data were used to produce cloud cover maps.

2.1.3 Soil and terrain

The SOTER soil and terrain database holds data for mapping units identified by distinctive patterns of landform, slope, lithology (soil parent material), and soils. Each SOTER unit is considered a unique combination of terrain and soil characteristics (van Engelen and Wen 1995, Dijkshoorn and others 2008). A SOTER at 1:1 million scale was compiled for China first: terrain units were sub-divided and characterized according to parent material and soil properties. The SOTER landform is based on the 90 m digital elevation data of the Shuttle Radar Topography Mission (SRTM, CGIAR-CSI 2004): single-parameter maps were derived for elevation, slope and relief intensity; a combination of these parameters is used to generate terrain units. Soil information was derived from the digital *Soil Map of China* compiled in 1995 by the Institute of Soil Science, Chinese Academy of Sciences from data of the Office for the Second National Soil Survey of China (Shi and others 2004). The digital soil map has a raster format of 30 arc seconds (approximately 1 km); mapping units are based on the genetic soil classification of China with soil family being the lowest categorical unit; this was correlated with the FAO Revised Legend (FAO-UNESCO 1988). The initial China SOTER, containing more than 67000 polygons, was generalized by dissolving all polygons smaller than 10 km^2, merging adjacent units that have similar attributes and, finally, by eliminating polygons smaller than 50 km^2.

2.1.4 Land cover and land use

Global Land Cover 2000 data (JRC 2003) and land use systems (FAO 2008) have been used for the comparison with NDVI trends.

Land use data for Zhejiang Province in 1985 and 2005, derived from Landsat TM imagery, were used to analyze the influence of land use change on land degradation. MODIS 16-day NDVI data at 500 m spatial resolution for 2004 were used to derive stable values of NDVI of different land use types.

2.2 Methods and Analysis

1. For each pixel, the annual sum NDVI is taken to represent annual accumulated greenness; HANTS is applied to GIMMS NDVI data to exclude extreme values and emphasize the underlying trends; 26-year trends were generated by linear regression.

2. Rain-use efficiency (RUE) is used to separate NDVI trends caused by drought by:
   - Identifying areas where rainfall determines biomass productivity (those pixels where there is a positive relationship between productivity and rainfall);
   - For these areas, where NDVI declined but RUE increased, we attribute declining productivity to declining rainfall and such areas are masked;
   - For the remaining areas, i.e. those with a positive relationship between productivity and rainfall but declining RUE and, also, all areas where rainfall does not determine productivity (where there is a negative relationship between NDVI and rainfall), NDVI trend has been calculated as RUE-adjusted NDVI.

   A negative trend of RUE-adjusted NDVI is taken as a proxy for land degradation.

3. Similarly, energy-use efficiency (EUE) is used to separate NDVI trends caused by rising temperature.

4. Areas considered to be improving are identified by both a positive trend of sum NDVI and positive RUE and EUE, referred to as climate-adjusted NDVI.

5. The *t*-test was used to test the confidence of the linear regression: t = b/Sb where b is the estimated slope of the regression line between the observation values and time and Sb represents the standard error of b. Class boundaries were defined for 95% levels.

6. Translation of NDVI trend to loss of NPP: to get a measure open to economic analysis, the NDVI time series has been translated to NPP using MODIS data (Justice and others 2002, Running and others 2004)[1] for the overlapping period 2000-2006: NPP was estimated by correlation with MODIS 8-day NPP values for the overlapping years of the GIMMS and MODIS datasets (2000-2006), re-sampling the annual mean MODIS NPP at 1 km resolution to 8 km resolution using nearest-neighbour assignment.

7. Analysis of residuals from the trend of each SOTER unit (RESTREND-SOTER) as a whole has been performed to take account of the effects of soil and terrain on the land's resilience to degradation:
   - The annual mean NDVI of the SOTER unit from 1981 to 2006 was calculated and re-sampled to the same pixel size as GIMMS.
   - Residuals of annual NDVI (difference between the annual sum NDVI and the annual mean NDVI based on SOTER unit) were calculated for each pixel.

---

[1] MOD17A3 is a dataset of terrestrial gross and net primary productivity computed at 1-km resolution and an 8-day interval. Though far from perfect (Plummer 2006), MODIS gross and net primary productivity values are related to observed atmospheric CO_2 concentrations and the inter-annual variability associated with the ENSO phenomenon, indicating that the NPP data are reliable at the regional scale (Zhao and others 2005, 2006). The dataset has been validated in various landscapes (Fensholt and others 2004, 2006, Gebremichael and Barros 2006, Turner and others 2003, 2006).

- The trend of these residuals was analyzed by linear regression.
- This is different from the RESTREND procedure of Wessels and others (2007).

8. The indices of land degradation and improvement were compared with land cover, land use and landform.

9. For Zhejiang Province, the influence of land use change on land degradation was analyzed using existing land use maps derived from Landsat data in 1985 and 2005.
   - Sum MODIS NDVI values in 2004 were calculated and mean sum MODIS NDVI values of each land use types were extracted with the Zonal Statistics command in ArcGIS 9.3;
   - Based on the mean sum MODIS NDVI value and the area weights of every land use type, the NDVI value for 1985 and 2005 was calculated for every pixel;
   - The trend of RUE-adjusted NDVI at 95% confidence level is compared with numerical change in NDVI ascribed to land use change between 1985 and 2005.

This method is summarized in Figure 1.
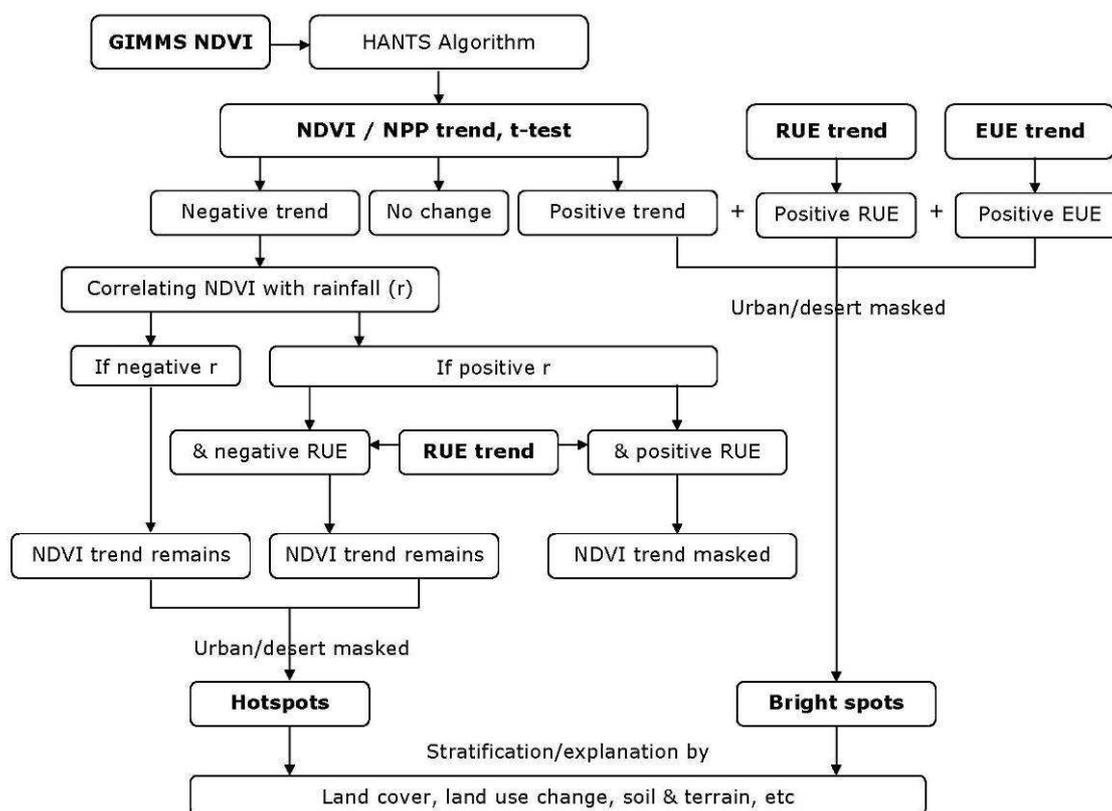
NDVI: Normalized Difference Vegetation Index; NPP: Net Primary Productivity; RUE: Rain-Use Efficiency; EUE: Energy-Use Efficiency

Figure 1. Flow chart for mapping proxy of land degradation and improvement.

3   Results and discussion

3.1   NDVI trends

Figure 2 shows the NDVI trends of the whole country, over the period 1981-2006.
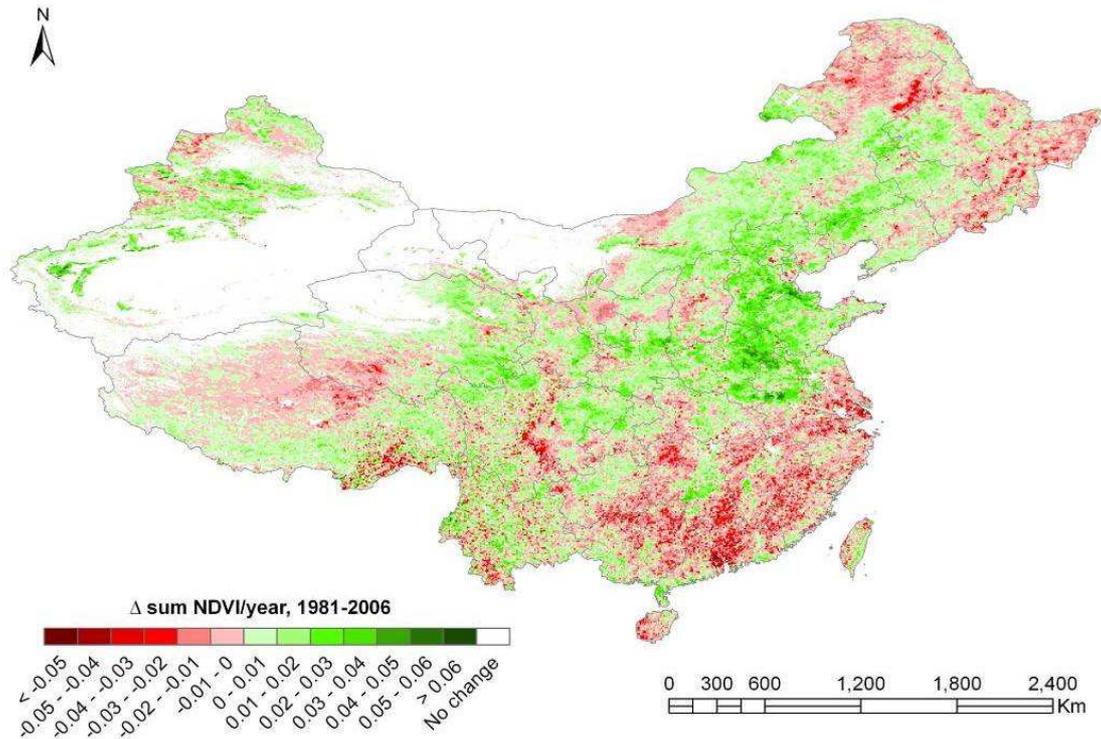
**Figure 2. NDVI trend 1981-2006, slope of sum NDVI linear regression**

Forty five percent of the country showed a positive NDVI trend (only 17% at significance level, *P*<0.05); 32% of the country suffered a negative trend (7% at significance level, *P*<0.05); 23% of the country is ice, extreme desert or inland water which have very low NDVI values and are designated as no change (Figure 3 and Table 1).
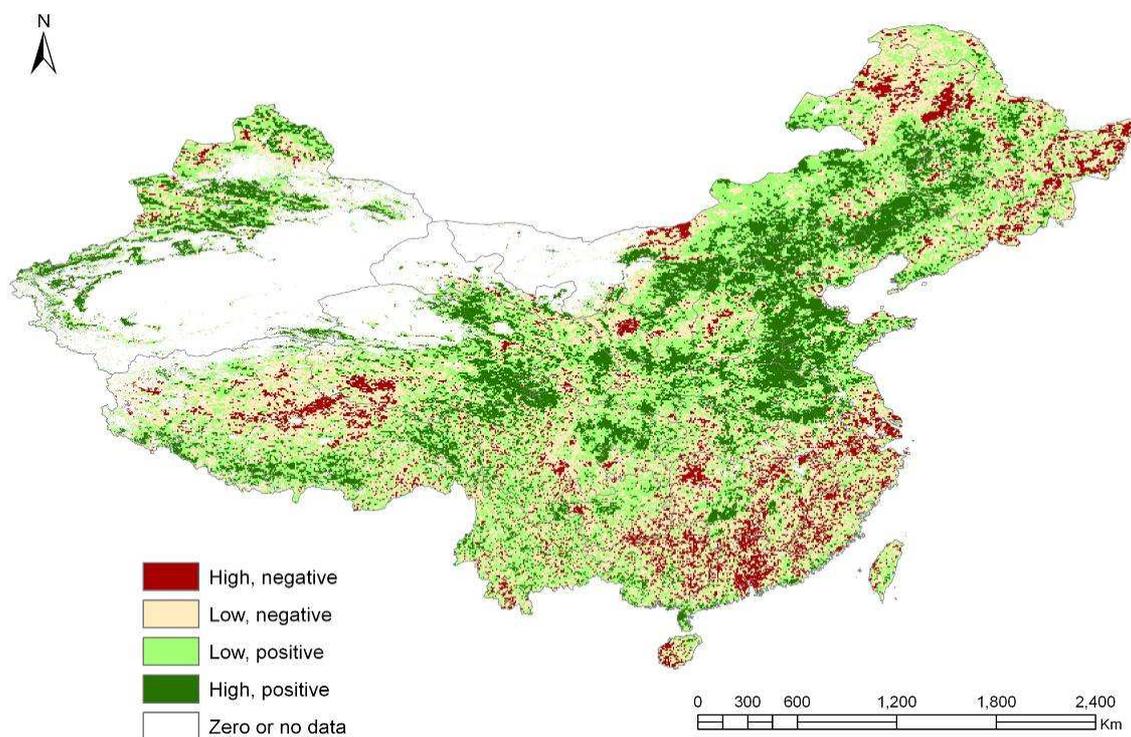
Figure 3. Confidence levels of NDVI trends, 1981-2006
         (High: at 95% confidence level)

Table 1.   Statistics of NDVI trends, all pixels

	NDVI		Total	Positive	Negative	No change
NDVI trends	all	Pixels	181 767	82 256	58 119	41 392
		%	100	45.2	32	22.8
	at 95% confidence level	Pixels	43 985	30 507	13 478	
		%	24.2	16.8	7.4	
RUE-adjusted NDVI	all	Pixels		31 658	42 711	
		%		17.4	23.5	
	at 95% confidence level	count			10 100	
		%			5.6	
Climate-adjusted NDVI	all	Pixels		31 308		
		%		17.2		
	at 95% confidence level	Pixels		13 409		
		%		7.4		

3.2   Negative RUE-adjusted NDVI

For those pixels with positive correlation between NDVI and rainfall and positive RUE trend, declining greenness (negative NDVI trend) is attributed to decreasing rainfall. The remaining areas of declining NDVI are shown as RUE-adjusted negative NDVI. Figure 4 depicts the trend as an absolute decline in NDVI and Figure 5, as a percentage decline.
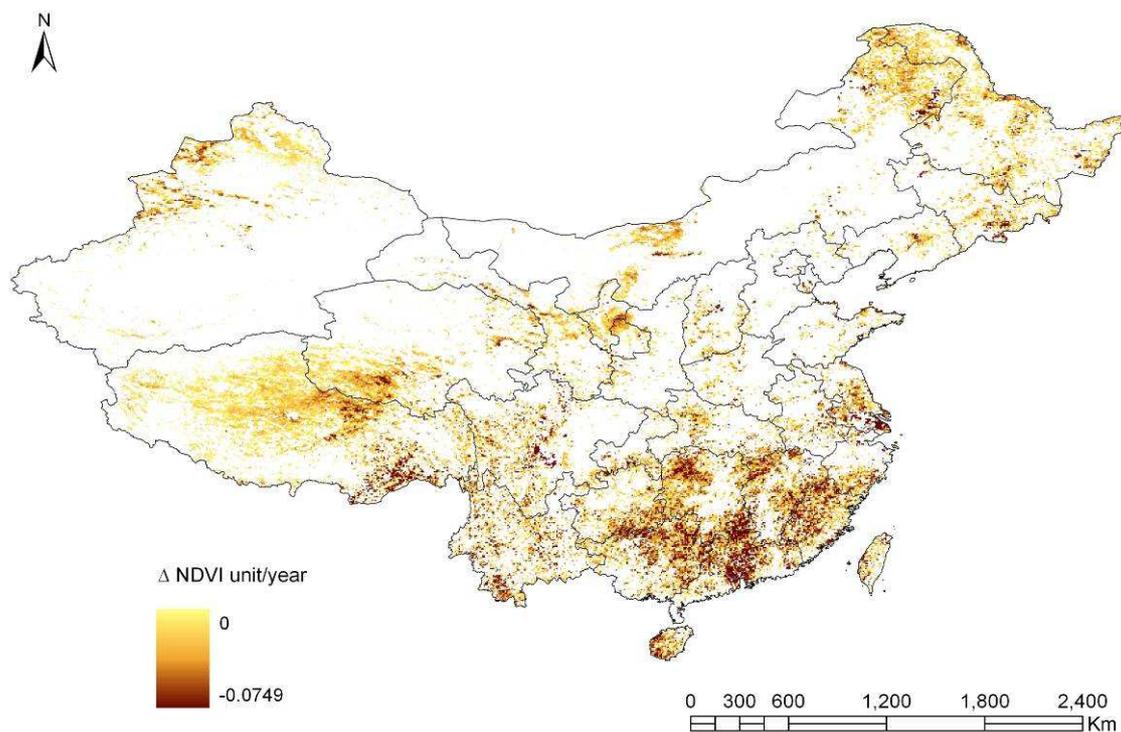
Figure 4. Negative trend in RUE-adjusted NDVI, 1981-2006 (absolute decline)
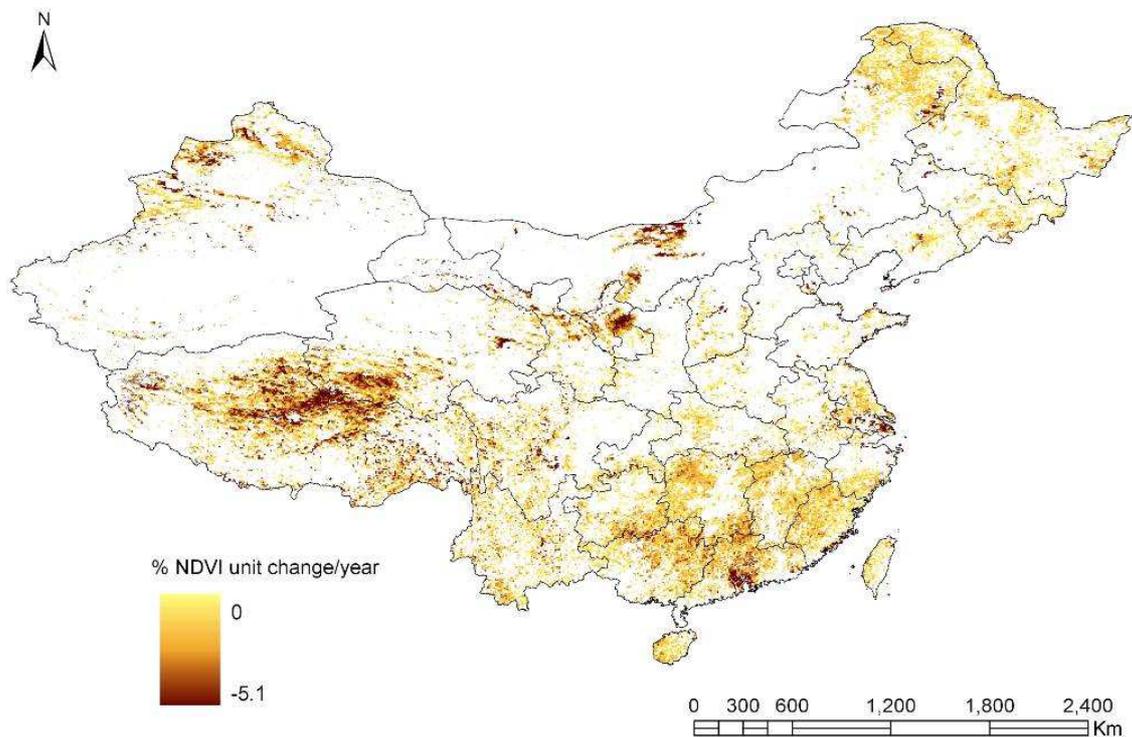
Figure 5. Negative trend in RUE-adjusted NDVI, 1981-2006 (percentage decline)

By this calculation, 24% of the country suffered negative RUE-adjusted NDVI. This is almost identical to the results of Bai and Dent (2009) using 1981-2003 GIMMS data. We may conclude that their preliminary analysis was unaffected by cloud effects. The area masked, where declining NDVI is attributed to a long-term decline in rainfall, comprises 8.5% of the country (Table 1).

Figure 6 shows 95% confidence levels of the negative trends in NDVI.
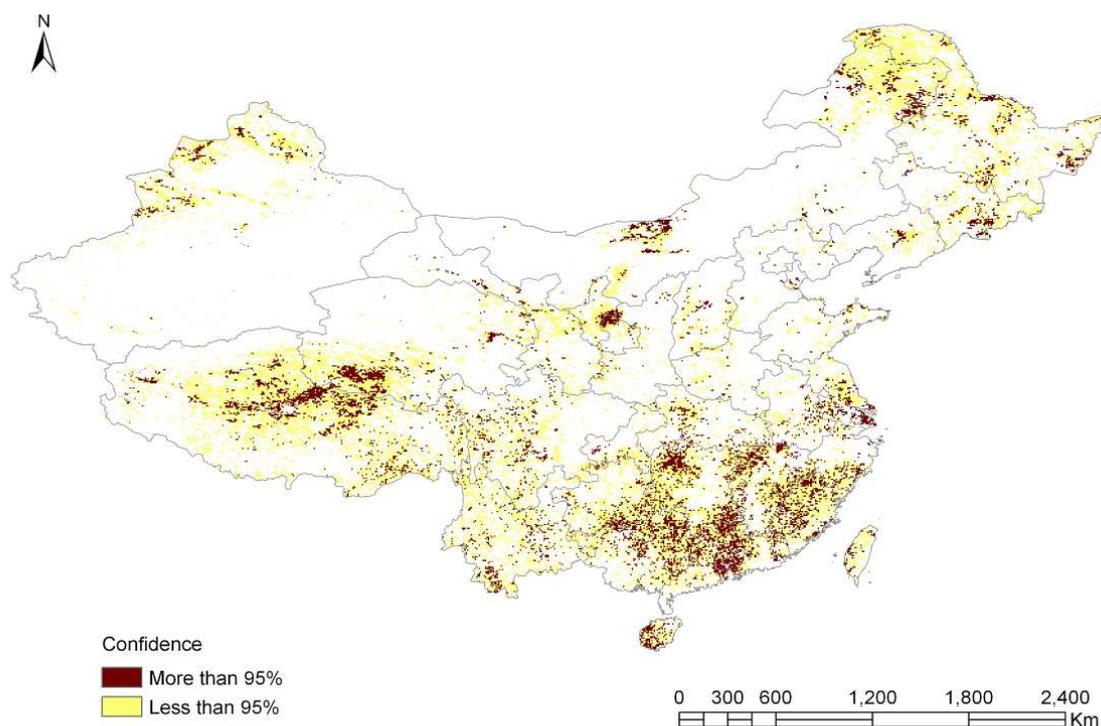
Figure 6. Confidence levels of RUE-adjusted NDVI, 1981-2006

Only 6% of the country shows a negative trend at 95% confidence level. This small area may be explained by the coarse resolution of the GIMMS data (8 km); degradation of an area much smaller than 8 km across must be severe to significantly change the signal from a much larger surrounding area. We may deduce that *hot spots* of land degradation identified with 95% confidence include significant areas with severe land degradation or large areas with some measurable degradation. These figures indicate that south China (especially in the Pearl River delta), North-east China, the Yangtze River delta, and the central of Tibetan Plateau are most affected by land degradation.

Figure 7 shows loss of net primary productivity in China during the period 1981-2006.
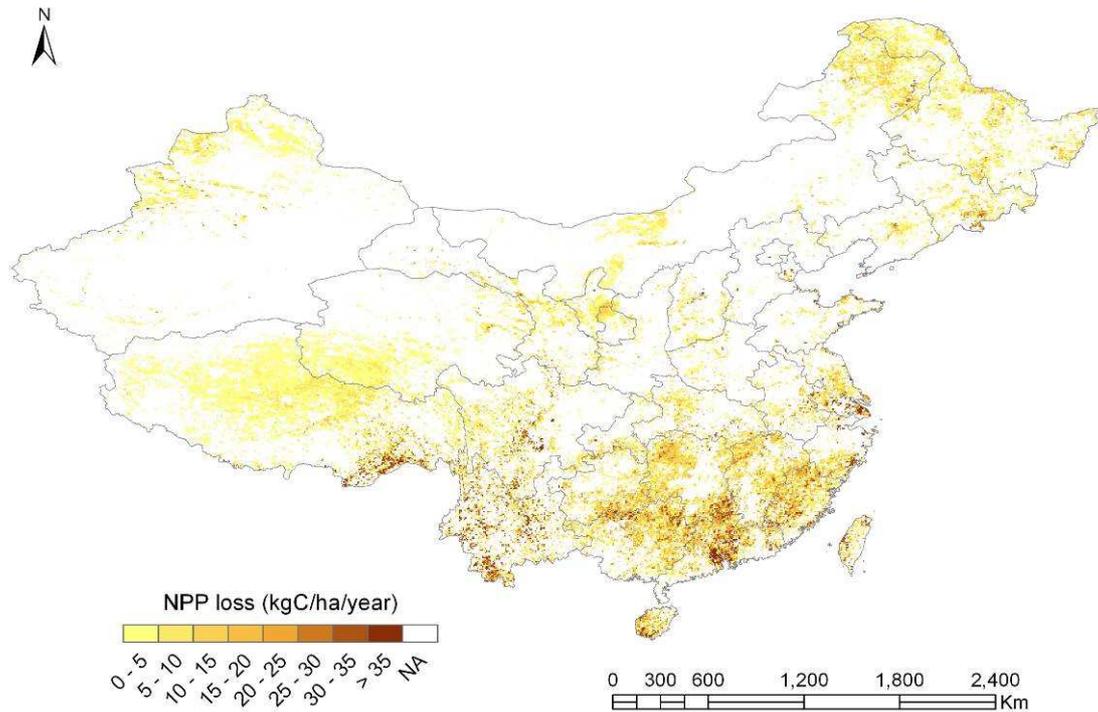
Figure 7. Loss of NPP, 1981-2006

3.3   Climate-adjusted NDVI

Improving land is identified by a positive RUE-adjusted NDVI and positive EUE (Figures 8 and 9). For China, correction for energy-use efficiency makes hardly any difference. A positive NDVI trend is observed for 45% of the country; 17.4% a positive RUE-adjusted NDVI; and 17.2% a positive climate-adjusted NDVI (7.4% at 95% confidence level) (Table 1 and Figure 10).
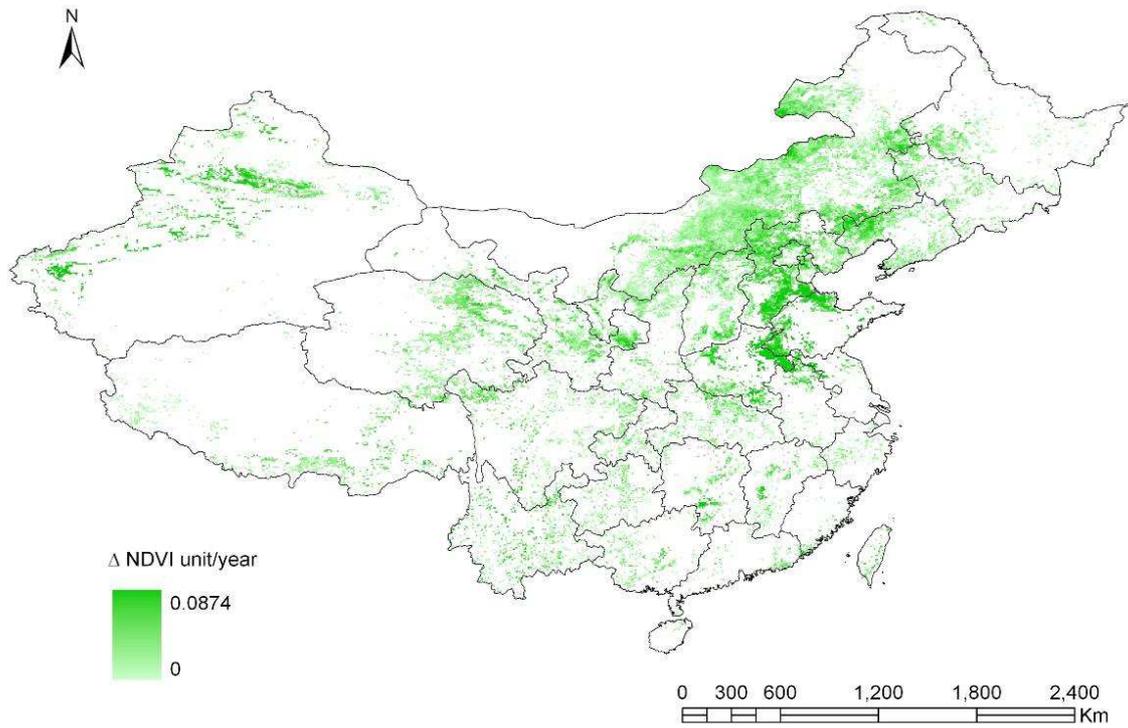
Figure 8. Positive climate-adjusted NDVI trend, 1981-2006 (absolute change)
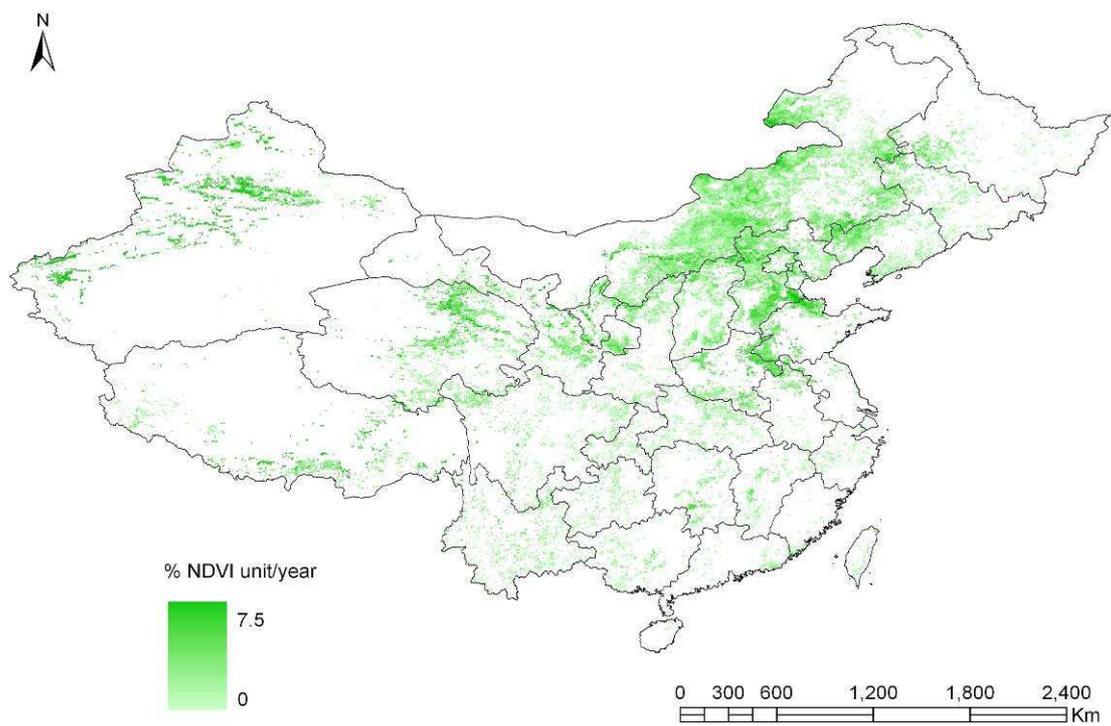
Figure 9. Positive climate-adjusted NDVI trend, 1981-2006 (percentage change)
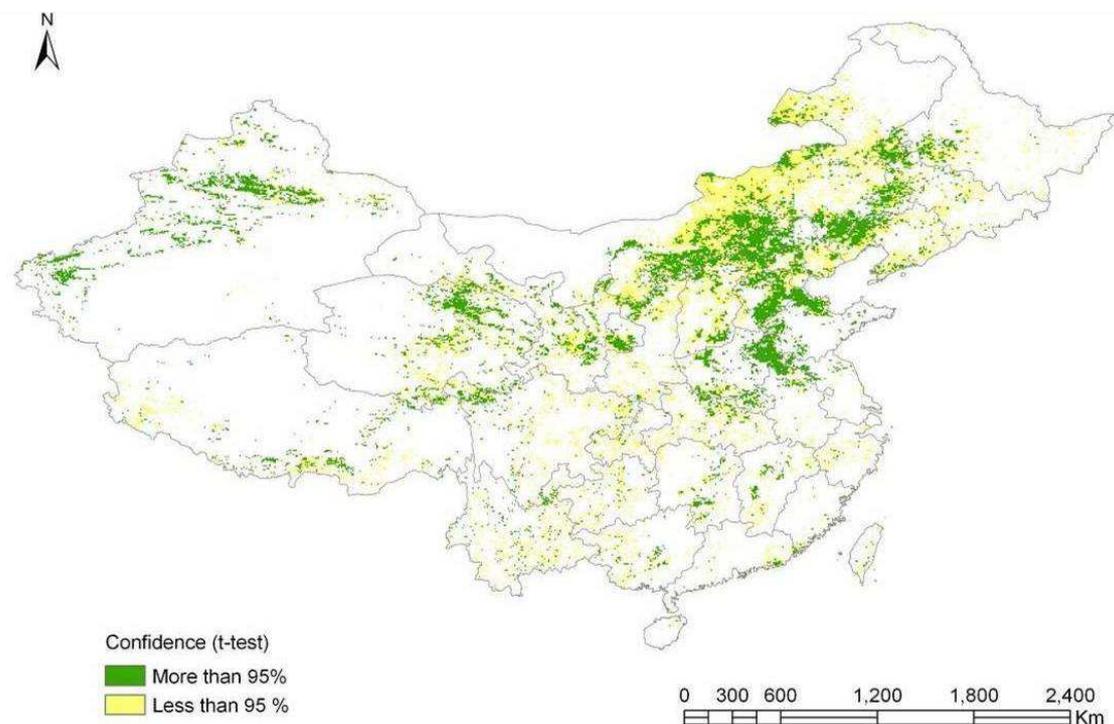
Figure 10. Confidence levels of climate-adjusted NDVI, 1981-2006

The area of improving climate-adjusted NDVI 1981-2006 accounts for 17% of the country; twice the area calculated by Bai and Dent (2008) based on NDVI 1981-2003. MODIS NDVI data from 2000 to 2006 also show an increased area with positive NDVI trend, which may indicate real improvement in biomass productivity in recent years, probably related to increased soil, water and vegetation conservation efforts.

Areas masked on account of long-term increasing rainfall comprise 28% of the country; areas masked on account of increasing temperature only 0.2%.

3.4   Land cover and land use systems of the degrading and improving areas

Comparison of degrading areas with land cover shows that about half of all forest land has been degrading; forests comprise 35% of the degrading area. Seventeen percent of cropland and 34% of mosaic cropland with other land cover is degrading; cropland comprises 14% of degrading land. About 28% of grassland and sparse scrub is degrading; these areas comprise 34% of the degrading area.

Of the improving area, 30% is cropland (code 16) and 17% mosaic cropland (code 17-18), 21% is grassland (code 13-14), 17% is closed deciduous broadleaved forest (Table 2). Forests comprise 15% of the improving area – 12% the total forest.

Comparison of degrading areas with land use systems (FAO 2008, Tables 3 and 4) indicates that 33% of degrading land is forest – 40% of the total forest: about half of plantations, 45% of natural and protected forests, 36-38% of grazed forests in China. Forty one percent of the degrading area is grasslands (herbaceous vegetation in the FAO legend) – 27% of the total grasslands. Sixteen percent of degrading area is agricultural land, which makes up 19% of the total agricultural land. A similar percentage is shown in the GLC2000 land cover. Areas with irrigation and protection are hardly better than the average.

As the improving areas are concerned, 43% is grassland, 34% is agricultural land, 14% is forestry and 6 % is bare land. Interestingly, grazed grassland appears to perform better than natural and protected grassland; large scale irrigation and protected areas of agricultural lands show no better results than other agricultural land. But for forestry, natural and protected areas show higher percentages of improving areas than pastoral areas.

Change of land use and management may generate false alarms about perceived land degradation. Conversion of forest or grassland to arable, pasture or even perennial crops will usually result in an immediate reduction in NPP (and NDVI) but may well profitable and sustainable, depending on management.

The approach used above has certain limitations, as described in Bai and others (2008b). Most important though is the need for groundtruthing. The maps in this report only concern a change in biomass (as observed through NDVI trends) as an indicator for land degradation. Field verification should determine whether this change is real and what has been the cause.

Table 2.   Land cover of the degrading and improving lands

Code	Land cover	Total pixels	Degrading pixels (DP)			Improving pixels (IP)		
		(TP)	(DP)	DP/TP (%)	DP/TDP (%)	IP	IP/TP (%)	IP/TIP (%)
1	Tree Cover, broadleaved, evergreen	443 913	220 272	49.6	7.8	43 610	9.8	2.1
2	Tree Cover, broadleaved, deciduous, closed	681 660	182 114	26.7	6.4	114 629	16.8	5.5
3	Tree Cover, broadleaved, deciduous, open	363	108	29.8	0.0	11	3.0	0.0
4	Tree Cover, needle-leaved, evergreen	1035 212	420 180	40.6	14.9	125 721	12.1	6.1
5	Tree Cover, needle-leaved, deciduous	244 575	123 404	50.5	4.4	8 778	3.6	0.4
6	Tree Cover, mixed leaf type	15 713	7 311	46.5	0.3	658	4.2	0.0
9	Mosaic: Tree Cover / Other natural vegetation	106 764	38 627	36.2	1.4	13 898	13.0	0.7
10	Tree Cover, burnt	944	505	53.5	0.0	63	6.7	0.0
11	Shrub Cover, closed-open, evergreen	551 446	238 886	43.3	8.4	100 027	18.1	4.8
12	Shrub Cover, closed-open, deciduous	15 702	5 437	34.6	0.2	810	5.2	0.0
13	Herbaceous Cover, closed-open	3 173 203	879 132	27.7	31.1	640 857	20.2	30.9
14	Sparse herbaceous or sparse shrub cover	760 114	82 684	10.9	2.9	192 762	25.4	9.3
15	Regularly flooded shrub and/or herbaceous cover	59 354	16 532	27.9	0.6	6 717	11.3	0.3
16	Cultivated and managed areas	2 242 026	380 207	17.0	13.4	666 085	29.7	32.1
17	Mosaic: Cropland / Tree Cover / Other natural vegetation	27 474	12 079	44.0	0.4	2 662	9.7	0.1
18	Mosaic: Cropland / Shrub and/or grass cover	103 572	31 961	30.9	1.1	19 243	18.6	0.9
19	Bare Areas	2 262 000	136 057	6.0	4.8	105 400	4.7	5.1
20	Water Bodies	172 920	29 757	17.2	1.1	19 735	11.4	1.0
21	Snow and Ice	155 485	19 708	12.7	0.7	9 985	6.4	0.5
22	Artificial surfaces and associated areas	6 936	2 784	40.1	0.1	739	10.7	0.0
23	No data	900	137	15.2	0.0	0	0.0	0.0
	Total	12 060 276	2 827 882	23.4	100.0	2 072 390	17.2	100.0

Pixel size: 0.0089° by 0.0089°, TDP: total degrading pixels, TIP: total improving pixels.

Table 3.   Degrading and improving areas by land use systems

Code	Land use systems	Total pixels (TP) (5'×5')	Degrading Pixels (DP) (5'×5')	DP/TP (%)	DP/TDP[1] (%)	Improving Pixels (IP) (5'×5')	IP/TP (%)	IP/TIP[2] (%)
1	Forestry - no use / not managed (Natural)	9 636	4 287	44.5	13.2	684	7.1	2.9
2	Forestry - Protected areas	1 637	730	44.6	2.3	128	7.8	0.5
4	Forestry - Pastoralism moderate or higher	15 214	5 451	35.8	16.8	2 315	15.2	9.7
5	Forestry - Pastoralism moderate or higher with scattered plantations	496	190	38.3	0.6	68	13.7	0.3
6	Forestry - Scattered plantations	229	117	51.1	0.4	31	13.5	0.1
7	Herbaceous - no use / not managed (Natural)	8 846	2 186	24.7	6.7	871	9.8	3.6
8	Herbaceous - Protected areas	11 926	3 912	32.8	12.1	921	7.7	3.9
9	Herbaceous - Extensive pastoralism	9 855	2 506	25.4	7.7	2 091	21.2	8.7
10	Herbaceous - Mod. Intensive pastoralism	5 812	1 211	20.8	3.7	2 261	38.9	9.5
11	Herbaceous - Intensive pastoralism	13 102	3 518	26.9	10.8	4 005	30.6	16.8
13	Rainfed Agriculture (Subsistence / commercial)	4 006	862	21.5	2.7	1 115	27.8	4.7
14	Agro-pastoralism Mod. Intensive	2 143	364	17.0	1.1	773	36.1	3.2
15	Agro-pastoralism Intensive	11 638	1 956	16.8	6.0	3 512	30.2	14.7
16	Agro-pastoralism mod. intensive or higher with Large scale irrigation	7 716	1 318	17.1	4.1	2 251	29.2	9.4
17	Agriculture - Large scale irrigation (> 25% pixel size)	2 010	512	25.5	1.6	360	17.9	1.5
18	Agriculture - Protected areas	581	173	29.8	0.5	114	19.6	0.5
19	Urban areas	3 798	984	25.9	3.0	861	22.7	3.6
20	Wetlands - no use / not managed (Natural)	403		0.0	0.0		0.0	0.0
21	Wetlands - Protected areas	62	69	111.3	0.2	78	125.8	0.3
24	Bare areas - no use / not managed (Natural)	16 912	450	2.7	1.4	281	1.7	1.2
25	Bare areas - Protected areas	3 239	382	11.8	1.2	79	2.4	0.3
26	Bare areas - Extensive pastoralism	5 919	740	12.5	2.3	583	9.8	2.4
27	Bare areas - Mod. Intensive pastoralism or higher	1 745	264	15.1	0.8	377	21.6	1.6
28	Water - Coastal or no use / not managed (Natural)	40	5	12.5	0.0	8	20.0	0.0
29	Water - Protected areas	407	85	20.9	0.3	10	2.5	0.0
30	Water - Inland Fisheries	853	156	18.3	0.5	125	14.7	0.5
100	Undefined	3		0.0	0.0		0.0	0.0
	Total	138 228	32 428		100.0	23 902		100.0

[1]TDP - total degrading pixels, [2]TIP - total improving pixels

Table 4.   Degrading and improving lands in the aggregated land use systems

Code	Land use systems	Total pixels (TP) (5′×5′)	Degrading pixels (DP) (5′×5′)	DP/TP (%)	DP/TDP[1] (%)	Improving pixels (IP) (5′×5′)	IP/TP (%)	IP/TIP[2] (%)
1 - 6	Forestry	27 212	10 775	39.6	33.2	3226	11.9	13.5
7 - 11	Grassland	49 541	13 333	26.9	41.1	10 149	20.5	42.5
13 - 18	Agricultural land	28 094	5 185	18.5	16.0	8 125	28.9	34.0
19	Urban	3 798	984	25.9	3.0	861	22.7	3.6
20 - 21	Wetland	465	69	14.8	0.2	78	16.8	0.3
24 - 27	Bare areas	27 815	1 836	6.6	5.7	1 320	4.7	5.5
28 - 30	Water	1 300	246	18.9	0.8	143	11.0	0.6
100	Undefined	3	0	0.0	0.0	0	0.0	0.0
	Total	138 228	32 428			23 902		

[1] TDP- total degrading pixels, [2] TIP - total improving pixels.

3.5　　Soil and terrain

SOTER is used to analyze the relationship between land degradation and soil and terrain condition. Figure 11 shows the landforms of areas identified here as degrading areas. All landforms are affected; however, hills and mountains (SOTER units SH, SM, TH and TM in Table 5) show a larger area of degrading land. In contrast, plains and depressions (LD, LF, LL, LP and LP wet) have less (Figure 12).
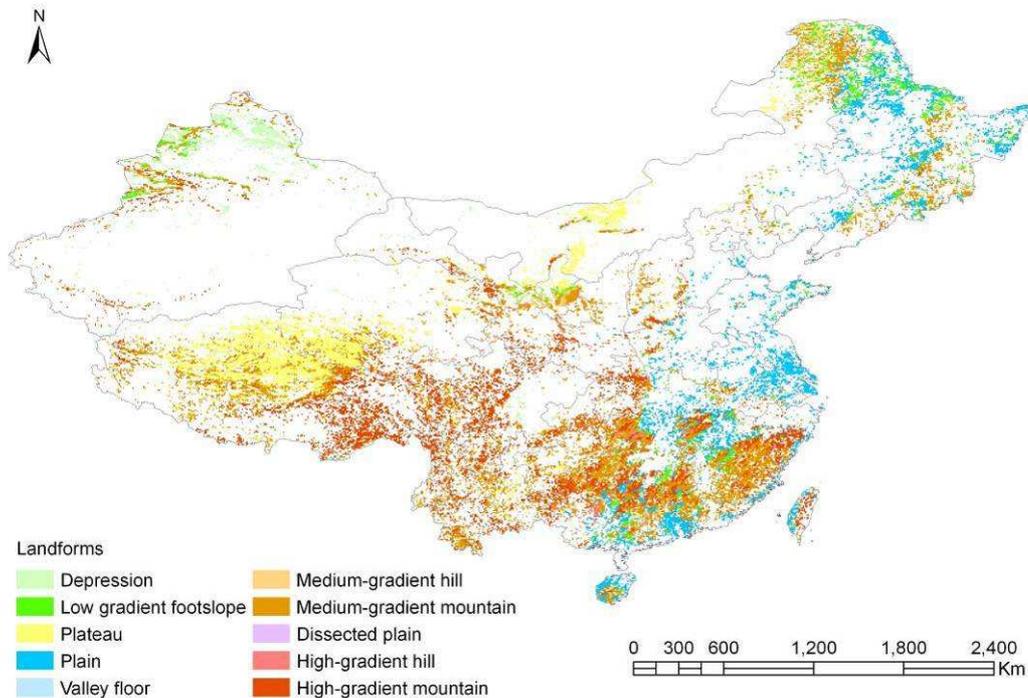

Figure 11. Areas of negative RUE-adjusted NDVI, 1981-2006, by SOTER landform

Table 6 presents the distribution of inferred degrading land in different slope classes. Less than a fifth of land with slopes less than 5% is degrading; a quarter to a third of slopes steeper than 5% are degrading. The picture is much the same at the 95% confidence level, except that there is less degradation on the steepest slopes (>35% slopes), which are more likely to be under natural vegetation (Figure 13).

Table 5.   Degrading areas by landforms

SOTER label	Landforms	Whole country		Inferred degrading land area			At 95% confidence level			Positive RESTREND-SOTER		Negative RESTREND-SOTER	
		WA	WA/ TWA	DL	DL/WA	DL/ TDL	DLS	DLS/ WA	DLS/ TDLS	PRL	PRL/ TPRL	NRL	NRL/ TNRL
		km²	%	km²	%	%	km²	%	%	km²	%	km²	%
LD	Depression	1 205 708	12.7	72 893	6.0	3.3	10 236	0.8	1.9	90	0.1	72 803	3.5
LF	Low-gradient foot slope	537 926	5.7	129 739	24.1	5.8	30 513	5.7	5.7	10 002	6.0	119 737	5.8
LL	Plateau	1 658 821	17.5	353 382	21.3	15.8	80 518	4.9	15.1	13 878	8.3	339 504	16.5
LP	Plain	1 590 940	16.8	351 822	22.1	15.8	106 509	6.7	19.9	23 169	13.9	328 653	15.9
LP Wet	Plain Wet	102 776	1.1	14 279	13.9	0.6	4 578	4.5	0.9	1 002	0.6	13 277	0.6
LV	Valley floor	138	0	56	40.5	0	12	8.6	0	8	0.0	48	0.0
SH	Medium-gradient hill	265 015	2.8	78 902	29.8	3.5	15 453	5.8	2.9	4 875	2.9	74 027	3.6
SM	Medium- gradient mountain	2 173 318	22.9	639 985	29.4	28.7	153 688	7.1	28.8	70 104	42.1	569 881	27.6
SP	Dissected plain	70 609	0.7	17 759	25.2	0.8	4 965	7.0	0.9	2 076	1.2	15 683	0.8
TH	High-gradient hill	122 186	1.3	40 042	32.8	1.8	11 311	9.3	2.1	3 625	2.2	36 417	1.8
TM	High-gradient mountain	1 761 988	18.6	531 156	30.1	23.8	116 536	6.6	21.8	37 497	22.5	493 659	23.9
	Total (TWA)	9 489 424	100	2 230 015	23.5	100	534 317	5.6	100	166 326	100.0	2 063 689	100.0

WA - area of landform unit, TWA - total area, DL – degrading area, TDL - total DL, DLS - degrading area at 95% confidence level, TDLS - total DLS, PRL - area of positive RESTREND SOTER, TPRL - total PRL, NRL – area of negative RESTREND SOTER, TNRL - total NRL

Table 6.   Degrading areas by slope classes*

Class	Slope	Whole country		Whole degrading land			At 95% confident level			Positive RESTREND-SOTER		Negative RESTREND-SOTER	
		TA	TA/TTA	DA	DA/TA	DA/TDA	DAS	DAS/TA	DAS/TDAS	PRS	PRS/TPRS	NRS	NRS/TNRS
	(%)	km²	%	km²	%	%	km²	%	%	km²	%	km²	%
1	0 - 0.5	102 776	1.1	14 279	13.9	0.6	4 577	4.5	0.8	1 002	0.6	13 277	0.6
2	0.5 - 2	2 456 255	25.9	352 557	14.4	15.4	95 539	3.9	17.3	15 116	9.1	337 441	16.4
3	2 - 5	1 580 323	16.7	306 466	19.4	13.4	76 727	4.9	13.9	18 179	10.9	288 287	14.0
4	5 - 10	956 953	10.1	248 867	26	10.9	55 520	5.8	10	13 852	8.3	235 015	11.4
5	10 - 15	158 114	1.7	55 842	35.3	2.4	10 474	6.6	1.9	3 864	2.3	51 978	2.5
6	15 - 30	2 350 827	24.8	680 803	29	30.5	163 631	7	30.6	73 191	44.0	607 612	29.4
7	30 - 45	983 201	10.4	340 108	34.6	14.9	90 839	9.2	16.4	35 781	21.5	304 331	14.7
8	> 45	900 972	9.5	231 089	25.6	10.1	37 007	4.1	6.7	5 341	3.2	225 748	10.9
Total (TTA)		9 489 424	100	2 230 015	23.5	100	534 317	5.6	100	166 326	100.0	2 063 689	100.0

* TA - area of slope class, TTA - total TA, DA - degrading area in slope class, TDA – total DA, DAS - degrading area in slope class at 95% confidence, TDAS – total DAS, PRS - area of positive RESTREND SOTER in slope class, TPRS – total PRS, NRS - area of negative RESTREND SOTER in slope class, TNRS – total NRS.
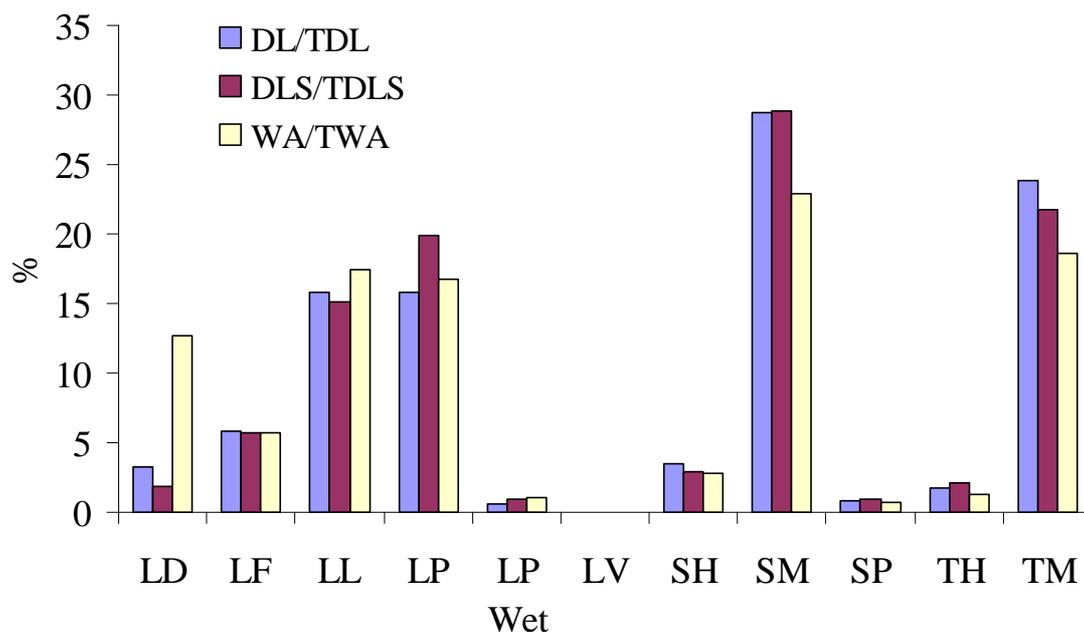
Figure 12. Percentage of degrading areas by landforms
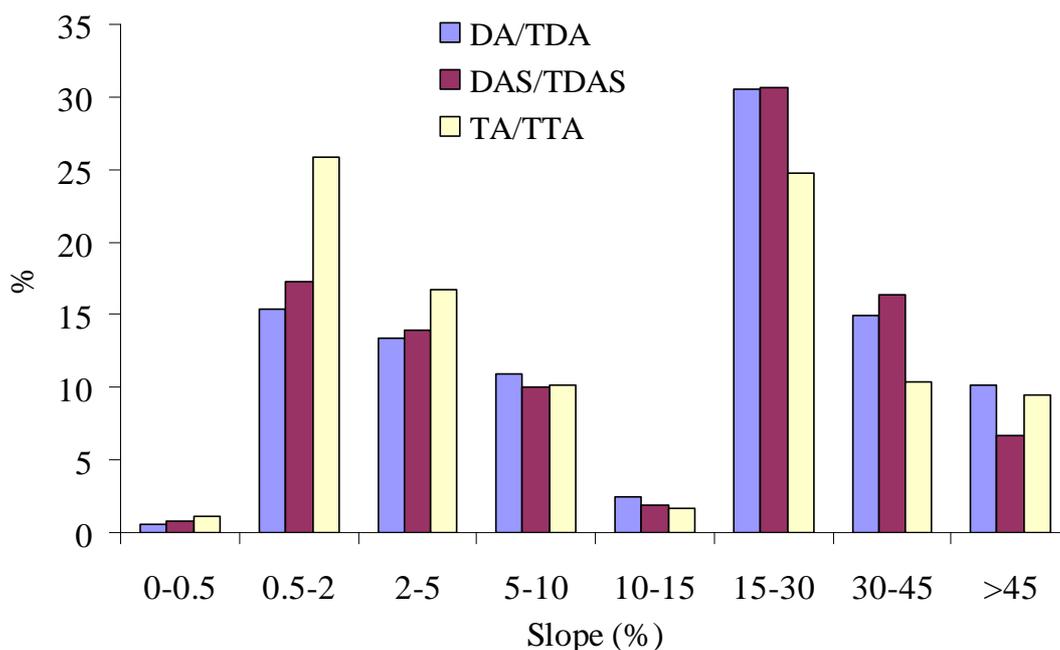

Figure 13. Percentage of degrading areas by slope classes

Figure 14 shows degrading areas by soil attributions. Over 70% of degrading area has less than 5% soil organic matter (SOM), and 25% of the area has SOM 5-10% (Figure 14a). However, degrading area appears over-represented in lower pH, i.e., <6.5, suggesting an influence of soil acidity on land degradation (Figure 14b). Figure 14c shows the distribution of degrading area by soil clay content (CLPC), classified as 0-15, 15-25, 25-45, 45-65 and >65%: the coarser the soil texture is, the easier it degrades. Degrading area is the most extensive in the soil clay contents of 15-45%, compared with whole country.
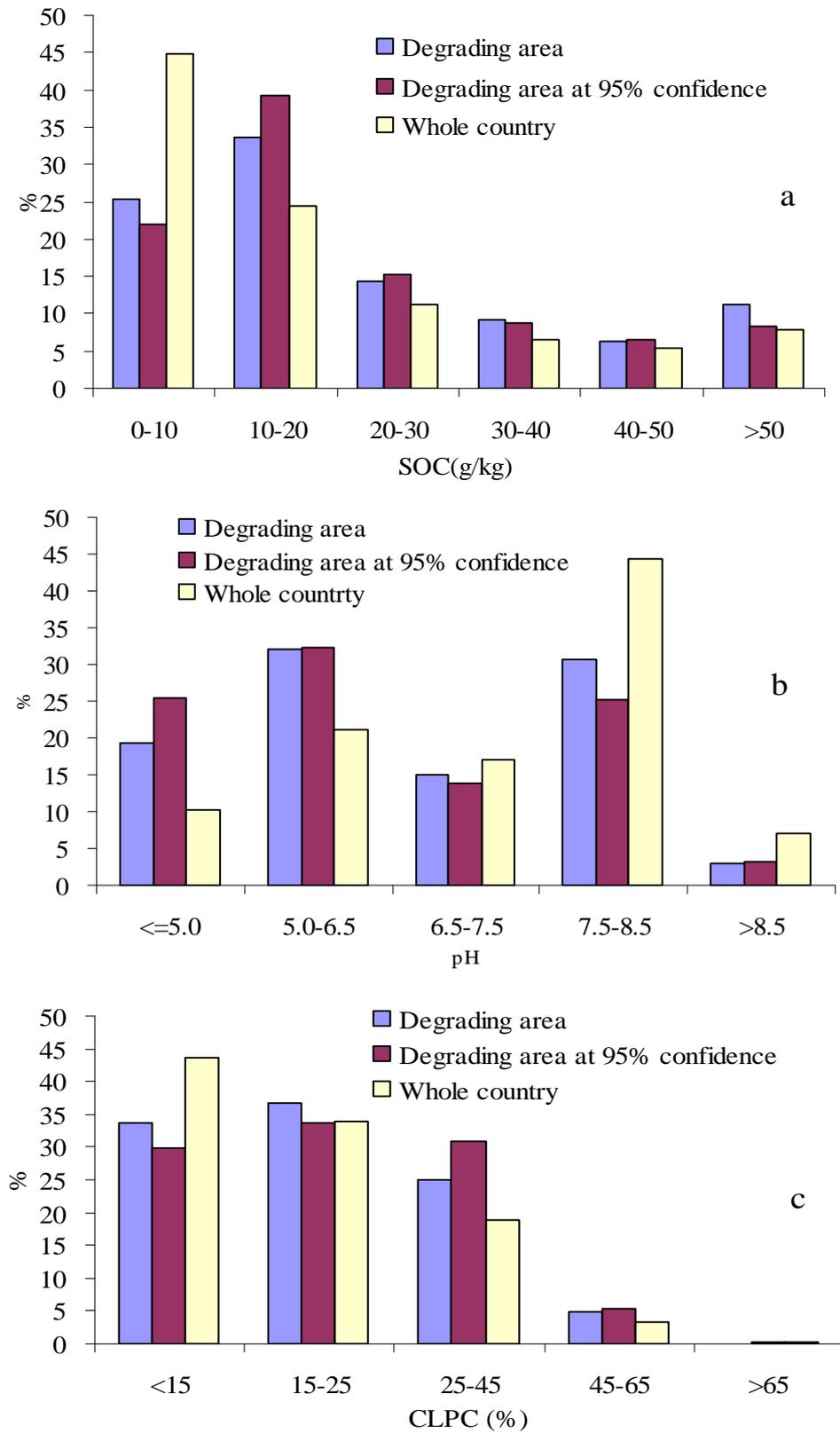
Figure 14. Distribution of degrading areas by soil attributes

3.6   RESTREND-SOTER

To take account of the influence of soil and terrain on derived land degradation, or resilience to degradation, each SOTER unit is analyzed independently and the trends of residual NDVI *within* SOTER units are analyzed pixel-by-pixel (RESTREND-SOTER). If SOTER units were homogeneous, this procedure would eliminate soil and terrain effects. They are not but, if the differences within the unit are less than those between units, we take some account of soil and terrain. Figure 15 depicts the trend of sum NDVI 1981-2006, based on SOTER units, i.e., trend of averaged sum NDVI within SOTER units. Figure 16 illustrates RESTREND-SOTER for the same period and Figure 17 the same data just for degrading areas as derived from the NDVI analysis.
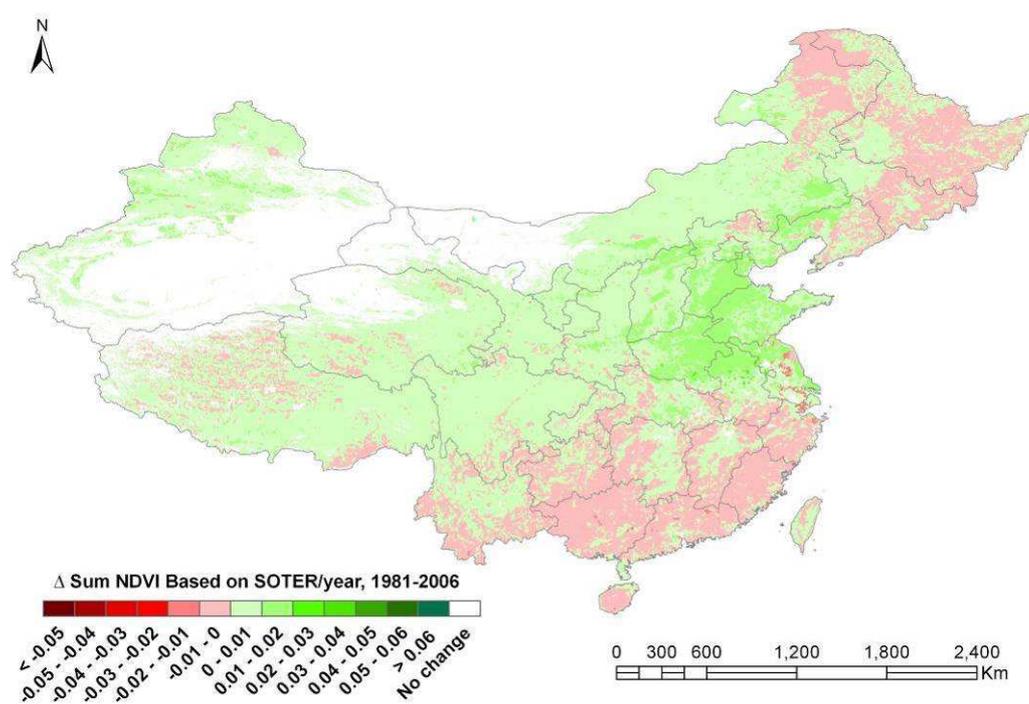
**Figure 15. Change in sum NDVI 1981-2006, by SOTER units, slope of linear regression**
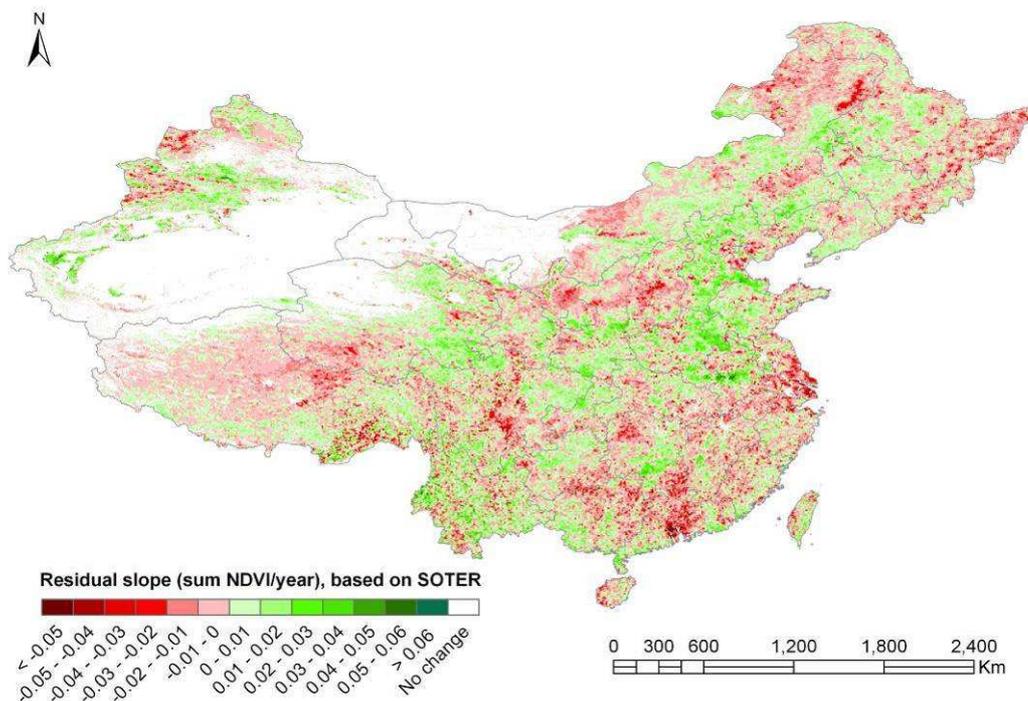
**Figure 16. Trends of NDVI residuals 1981-2006, RESTREND SOTER**
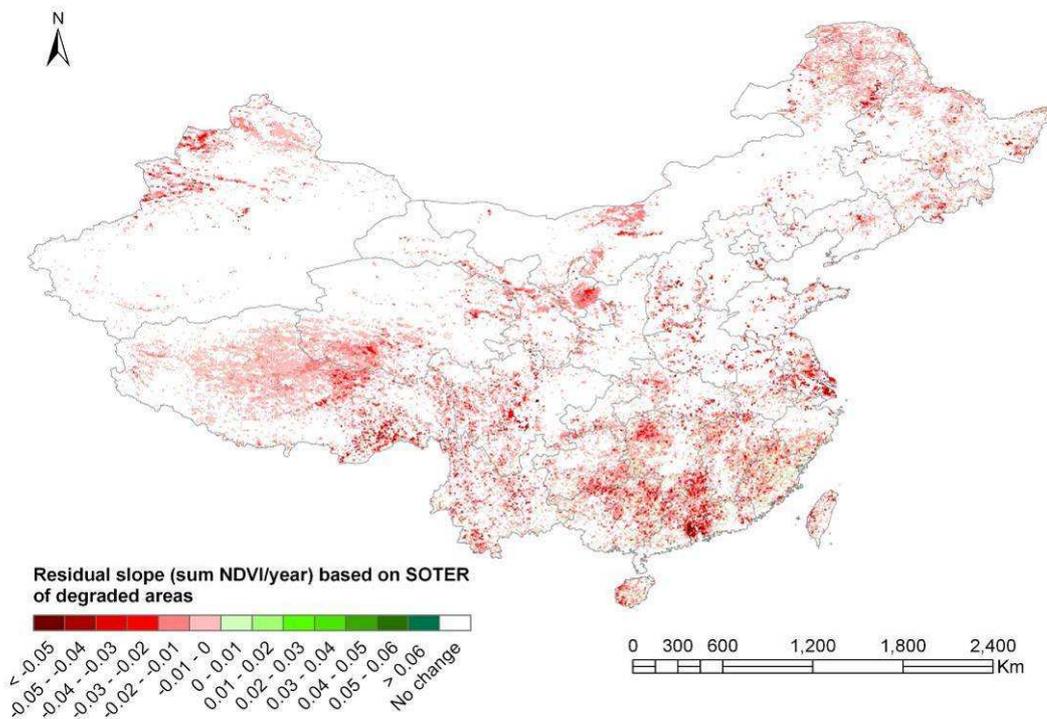
Figure 17. RESTREND-SOTER for degrading areas 1981-2006

The new product shows a relative departure from the NDVI trend from that of its landscape (the SOTER unit). It gives a different perspective on *hot spots* and *bright spots* from the previous pixel by pixel analysis of NDVI trends but does not supplant the absolute measure given by the climate-adjusted NDVI/NPP. Tables 5 and 6 present the areas of degrading land with positive RESTREND-SOTER and negative RESTREND-SOTER, respectively.

About 8% of the degrading land, i.e. 1.8% of whole country, shows a positive RESTREND-SOTER: two-thirds is with slopes between 15-45% and 29% with slopes less than 10% (Table 6). The remaining degrading lands shows a negative RESTREND-SOTER: 42% of those areas is level land, 32% sloping land and 26% steep land (Table 5). These degrading areas could be attributed to improper land management. The RESTREND-SOTER analysis could separate the impact of soil and terrain from other factors. Land management could be the best explanation for the derived degradation. However, caution should be applied to such interpretations due to the intrinsic variability of the SOTER units.

The wide differences between the absolute values of degrading areas (Figures 2, 4 and 6) and the patterns of RESTREND-SOTER (Figures 15, 16 and 17 and Tables 5 and 6) suggest that soil resilience has a significant effect on outcomes, of the order of 25%. This figure was estimated by comparison between the absolute values of RUE-adjusted NDVI and the maps of RESTREND-SOTER patterns in ArcMap.

3.7   Relationships between NDVI trend and land use change

Since the 1980's, China has achieved unprecedented economic development with rapid industrialization and growth of towns and cities, and associated environmental degradation. Comparing the extent of urban areas with decline in RUE-adjusted NDVI, we assume that urbanization and associated development of infrastructure account for much of the biomass decline in rapidly developing areas, e.g. in the Yangtze River delta and Pearl River delta.

Figure 18 shows a more detailed analysis for Zhejiang Province, in south-east China. The trend of RUE-adjusted NDVI at 95% confidence level, at pixel level, on the vertical axis, is plotted against numerical change in NDVI ascribed to land use change between 1985 and 2005, on the horizontal axis (Figure 18a). Similarly, RESTREND-SOTER, on the vertical axis, is plotted against land use change, on the horizontal axis (Figure 18b).

The extension of points in the first quadrant (positive/positive) and third quadrant (negative-negative) indicates that there is a relationship between land use change and land degradation and improvement. Apparently contradictory trends (positive-negative) and the mass of pixels showing degradation without land use change may be explained by changes in management within the same land use type, and by ecosystem disturbance such as forest fire or outbreaks of pests and disease that cannot be identified from our data, but this needs to be confirmed by further research.
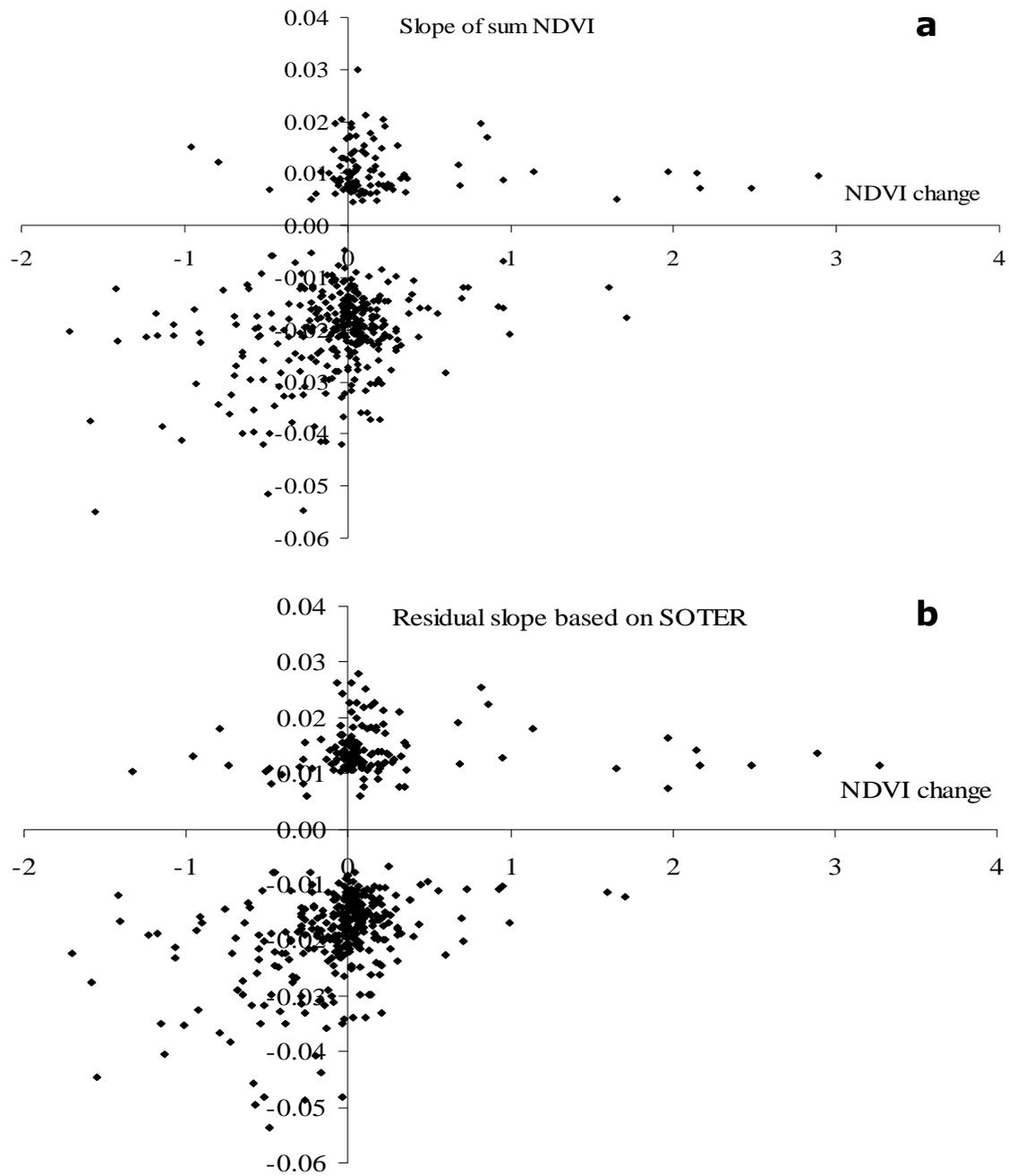
Figure 18. Relationship between NDVI changes ascribed to land use change and the slopes of sum NDVI of Zhejiang province

3.8   Relative effects of rainfall, temperature and land use change and soil/terrain on long-term NDVI trends

As a first approximation, we may estimate the relative influences of 26-year rainfall and temperature trends on biomass productivity from the areas masked according to decreasing NDVI but increasing rain use efficiency (drought effect), increasing NDVI but decreasing efficiency (increased rainfall effect), and increased NDVI but decreased energy-use efficiency (warming effect). For China as a whole, the drought effect explains 8.5% of the negative NDVI trend; increased rainfall explains 28% of the positive NDVI trend; increased temperature only 0.2% of the increased NDVI trend. What remains may be accounted for by land use change, of itself, and by land degradation and improvement brought about by changes in management.

The SOTER RESTREND analysis indicates that soil and terrain patterns affect the land's resilience to degradation, modifying the overall absolute change in NPP by about 25%.

4   Conclusions

- Over the period 1981-2006, 32% of the country exhibited a negative trend of NDVI and 45% a positive trend.

- Accounting for the influence of rainfall, 23.5% of the country exhibited negative RUE-adjusted NDVI.

- Taking account of rainfall and temperature, 7.4% of the country shows an increasing trend of climate-adjusted NDVI.

- Areas masked for RUE (8.5% of the country in negative NDVI trend, and 28% in positive NDVI trend) are considered to have trends explained by long-term rainfall trends, those masked for EUE (0.2% of the country) are explained by long-term temperature trends. The difference between the pixel-by-pixel pattern and the RESTREND-SOTER pattern (2% of the country) may be explained by soil and terrain effects.

- Countrywide, we have no data for the effects of land use change. From the partial analysis for Zhejiang Province, it appears that this is a significant driver of NDVI/NPP change. Probably more important than changes in land use are changes in management practices within the cropland, grazing land and forest categories, as well as unintentional events like fires and pest outbreaks – for which we do not have data.

Acknowledgements

References

Bai ZG, Dent DL, Olsson L and Schaepman ME 2008a Global assessment of land degradation and improvement. 1. Identification by remote sensing. Report 2008/01, ISRIC – World Soil Information, Wageningen

Bai ZG and DL Dent 2008b *Land degradation and improvement in China 1. Identification by remote sensing.* ISRIC Report 2007/6, ISRIC - World Soil Information, Wageningen

Bai ZG and DL Dent 2009 Recent land degradation and improvement in China. *AMBIO* 38, 150-156

Bai ZG, DL Dent, L Olsson and ME Schaepman 2008 Proxy global assessment of land degradation. *Soil Use and Management* 24, 223-234

Beck C, J Grieser and B Rudolf 2005 A new monthly precipitation climatology for the global land areas for the period 1950-2000. 181-190 in *Climate Status Report 2004*. German Weather Service, Offenbach

CGIAR-CSI 2004 *SRTM 90m Digital Elevation Data, Consortium for Spatial Information.* (http://srtm.csi.cgiar.org/SELECTION/inputCoord.asp accessed July 2008)

Dijkshoorn JA, VWP van Engelen and JRM Huting 2008 *Soil and landform properties for LADA partner countries (Argentina, China, Cuba, Senegal and The Gambia, South Africa and Tunisia).* ISRIC report 2008/06, ISRIC – World Soil Information, Wageningen

Engelen VWP van and Wen TT 1995 *Global and National Soil and Terrain Digital Database (SOTER) Procedures Manual*. ISRIC - World Soil Information, Wageningen

FAO 1979 *A Provisional Methodology for Soil Degradation Assessment.* FAO Rome

FAO 2008 *Land use systems of the World*. (http://www.fao.org/nr/lada/index.php?/LUS-map-zip-format/View-category.html, accessed 15 June 2008)

FAO-UNESCO 1988 *FAO/UNESCO Soil Map of the World, Revised Legend*. World Resources Report 60. Rome (ftp://ftp-anon.dwd.de/pub/data/gpcc/html/fulldata_download.html, accessed August 8 2008)

Fensholt R, I Sandholt and MS Rasmussen 2004 Evaluation of MODIS LAI, fAPAR and the relation between fAPAR and NDVI in a semi-arid environment using in situ measurements. *Remote Sensing of Environment* 91, 490-507

Fensholt R, I Sandholt, MS Rasmussen, S Stison and A Diouf 2006 Evaluation of satellite-based primary production modelling in the semi-arid Sahel. *Remote Sensing of the Environment* 105 173-188

Gebremichael M and AP Barros 2006 Evaluation of MODIS gross primary productivity (GPP) in tropical monsoon regions. *Remote Sensing of Environment* 100, 150–166

Hutchinson 1995 Interpolating mean precipitation using thin plate smoothing splines. *International Journal of Geographical Information Systems* 9, 385–403

Jong R de, ZG Bai, DL Dent, ME Schaepman, S de Bruin and A de Wit 2009 Enhanced assessment of global land degradation. Paper submitted for oral presentation on The 33rd International Symposium on Remote Sensing of Environment (ISRSE, 4-8 May 2009), Stresa, Italy

JRC 2003 *Global Land Cover 2000 database*. European Commission, Joint Research Centre (http://www-gemjrcit/glc2000, accessed 30 August 2006

Justice CO, JRG Townshend, EF Vermote, E Masuoka, RE Wolfe, N Saleous, DP Roy and JT Morisette 2002 An overview of MODIS Land data processing and product status. *Remote Sensing of Environment* 83, 3-15

McBeath JH and McBeath J. 2010 Environmental change and food security in China*. Advances in Global Change Research* 35, DOI 10.1007/978-1-4020-9180-3_10.

Millennium Ecosystem Assessment 2005 Living beyond our means: natural assets and human well-being. Statement from the Millennium Ecosystem Assessment Board (http://www.wri.org/publication/millennium-ecosystem-assessment-living-beyond-our-means-natural-assets-and-human-we)

Mitchell TD and PD Jones 2005 An improved method of constructing a database of monthly climate observations and associated high resolution grids. *International Journal of Climate* 25, 693-712

New M, D Lister, M Hulme, I Makin 2002 A high-resolution data set of surface climate over global land areas. *Climate Research* 21, 1–25

New M, M Hulme, PD Jones 1999 Representing twentieth century space–time climate variability. Part 1: development of a 1961–90 mean monthly terrestrial climatology. *Journal of Climate* 12, 829–856

New M, M Hulme, PD Jones 2000 Representing twentieth century space–time climate variability. Part 2: development of 1901–96 monthly grids of terrestrial surface climate. *Journal of Climate* 13, 2217–2238

Pinzon JE, ME Brown and CJ Tucker 2007 Global Inventory Modeling and Mapping Studies (GIMMS) Satellite Drift Corrected and NOAA-16 incorporated Normalized Difference Vegetation Index (NDVI), Monthly 1981–2006. Global Inventory Modeling and Mapping Studies (GIMMS) Satellite Drift Corrected and NOAA-16 incorporated Normalized Difference Vegetation Index (NDVI), Monthly 1981–2006. University of Maryland Global Land Cover Facility Data Distribution
(http://glcf.umd.edu/library/guide/GIMMSdocumentation_NDVIg_GLCF.pdf)

Plummer S 2006 On validation of the MODIIS gross primary production product. *IEEE Transactions on Geoscience and Remote Sensing* 44, 1936-1938

Roerink GJ, M Menenti and W Verhoef 2000 Reconstructing cloud-free NDVI composites using Fourier analysis of time series. *International Journal of Remote Sensing* 21, 1911-1917

Running SW, FA Heinsch, M Zhao, M Reeves and H Hashimoto 2004 A continuous satellite-derived measure of global terrestrial production. *Bioscience,* 54, 547-560

Schneider U, T Fuchs, A Meyer-Christoffer and B Rudolf 2008 *Global precipitation analysis products of the GPCC, full data re-analysis product version 4.* Global Precipitation Climatology Centre, German Weather Service, Offenbach

Shi XZ, DS Yu, ED Warner, XZ Pan, GW Petersen, ZG Gong and DC Weindorf 2004 Soil Database of 1:1,000,000 Digital Soil Survey and Reference System of the Chinese Genetic Soil Classification System. *Soil Survey Horizons* 45, 129-136

Tucker CJ, JE Pinzon and ME Brown 2004 *Global Inventory Modeling and Mapping Studies (GIMMS) Satellite Drift Corrected and NOAA-16 incorporated Normalized Difference Vegetation Index (NDVI), Monthly 1981-2002*. University of Maryland. (http://glcf.umd.edu/data/gimms/)

Turner DP, WD Ritts, WB Cohen, ST Gower, M Zhao, SW Running, SC Wofsy, S Urbanski, AL Dunn and JW Munger 2003 Scaling gross primary production (GPP) over boreal and deciduous forest landscapes in support of MODIS GPP product validation. *Remote Sensing of Environment* 88, 256–270

Turner DP, WD Ritts, WB Cohen, ST Gower, SW Running, M Zhao, MH Costa, AA Kirschbaum, JM Ham, SR Saleska, DE Ahl 2006 Evaluation of MODIS NPP and GPP products across multiple biomes. *Remote Sensing of Environment* 102, 282–292

UNEP 2007 *Global Environmental Outlook GEO-4, Chapter 3: Land.* UNEP, Nairobi

Verhoef W, M Menenti and S Azzali 1996 A colour-composite of NOAA-AVHRR-NDVI data based on time series analysis (1981-1992). *International Journal of Remote Sensing* 17, 231-235

Wessels KJ, SD Prince, J Malherbe, J Small, PE Frost and D VanZyl 2007 Can human-induced land degradation be distinguished from the effects of rainfall variability? A case study in South Africa*. Journal of Arid Environments* 68, 271-297

Wit AJW de and Su B 2005 Deriving phenological indicators from SPOT-VGT data using the HANTS algorithm. In, *2nd international SPOT-VEGETATION user conference* (pp. 195-201). Antwerp, Belgium

Zhao M, FA Heinsch, RR Nemani and SW Running 2005 Improvements of the MODIS terrestrial gross and net primary production global data set. *Remote Sensing of Environment* 95, 164-176

Zhao M, SW Running and RR Nemani 2006 Sensitivity of Moderate Resolution Imaging Spectroradiometer (MODIS) terrestrial primary production to the accuracy of meteorological reanalyses. *Journal of Geophysical Research* 111, G01002, doi:10.1029/2004JG000004

Appendix 1: Removal of Residual Cloud Effects

GIMMS NDVI data for 1981-2006 at 8km resolution are corrected for calibration, variations in solar view and zenith angle, volcanic aerosols and other effects not related to vegetation change (Tucker and others 2004, Pinzon and other 2007); we have used the HANTS algorithm (Verhoef and others 1996) to remove any residual cloudiness effects (de Jong and others 2009):

HANTS algorithm
Phenological patterns are extracted from GIMMS using the IDL-ENVI implementation of the HANTS algorithm (de Wit and Su, 2005). The basis of the algorithm is that seasonal effects in vegetation can be described using a limited number of low frequency sine functions with different phases, frequencies and amplitudes (Verhoef and others 1996). The HANTS algorithm, therefore, uses a Fourier analysis but complements the standard Fourier analyses with a detection of outliers which are flagged and replaced in an iterative approach. For this study, the algorithm has been configured according to Table A1. The base NDVI (Fourier component 0, FC0) and the yearly (FC1), 6-monthly (FC2) and 4-monthly (FC3) Fourier components were considered. The outlier detection has been configured such that it cannot reject more than one third of all data points and only points which deviate more than 0.1 (NDVI) from the fitted curve.

Table A1. Parameters used in HANTS

Parameters	Single-year	Full (26 years)
Number of points	24 (fortnightly)	624
Fourier frequencies	0,1,2,3	0,26,52,78
Minimal NDVI threshold	0.1	0.1
Maximum iterations	6	12
Maximum rejected data points	8	208

HANTS provides three main outputs: 1) an interpolated NDVI time-series, 2) a smoothed harmonic curve and 3) the contribution of each Fourier Component (FC) to the NDVI signal. The first contains the original NDVI values, with the outliers (original minus fitted>0.1) replaced by the fitted values. The second output contains the smoothed result – the harmonic analysis (HA) of the time-series. As HA is a mathematical approximation of the NDVI trend, it can be used to extract phenological indicators including Start of Season and End of Season and the amplitude and phase shift of the growing seasons. The third output consists of the individual FCs which are represented as complex numbers and can be converted into phase and amplitude which have a physical meaning.

The interpolated NDVI time series and Fourier Components were used in the subsequent analyses. To confirm/verify the effects of HANTS results, the CRU 3.0 monthly time series cloudiness data were used to produce cloud cover maps.

The CRU TS 3.0 dataset, created by the Climate Research Unit of the University of East Anglia, UK, comprises monthly grids of meteorological station-observed data for the period 1901-2006 covering the global land surface at 0.5 degree resolution. The data were collated from as many stations as possible to develop both monthly mean climatology (1961-1990) and time series (1901-2006) of various climate variables (New and others 1999, 2000, 2002), using thin-spline interpolation (Hutchinson 1995) with consideration of elevation effects. Data are available for: daily mean, minimum and maximum temperature; diurnal temperature range; precipitation, wet-day frequency; frost-day frequency; vapour pressure; and cloud cover (Mitchell and Jones 2005). Monthly temperature values since January 1981, gridded at 0.5° resolution were used to calculate the cloudiness.

Figure A1 shows cloud cover and numbers of GIMMS time series NDVI replaced using HANTS. It indicates that HANTS remove well residual cloudiness effects.
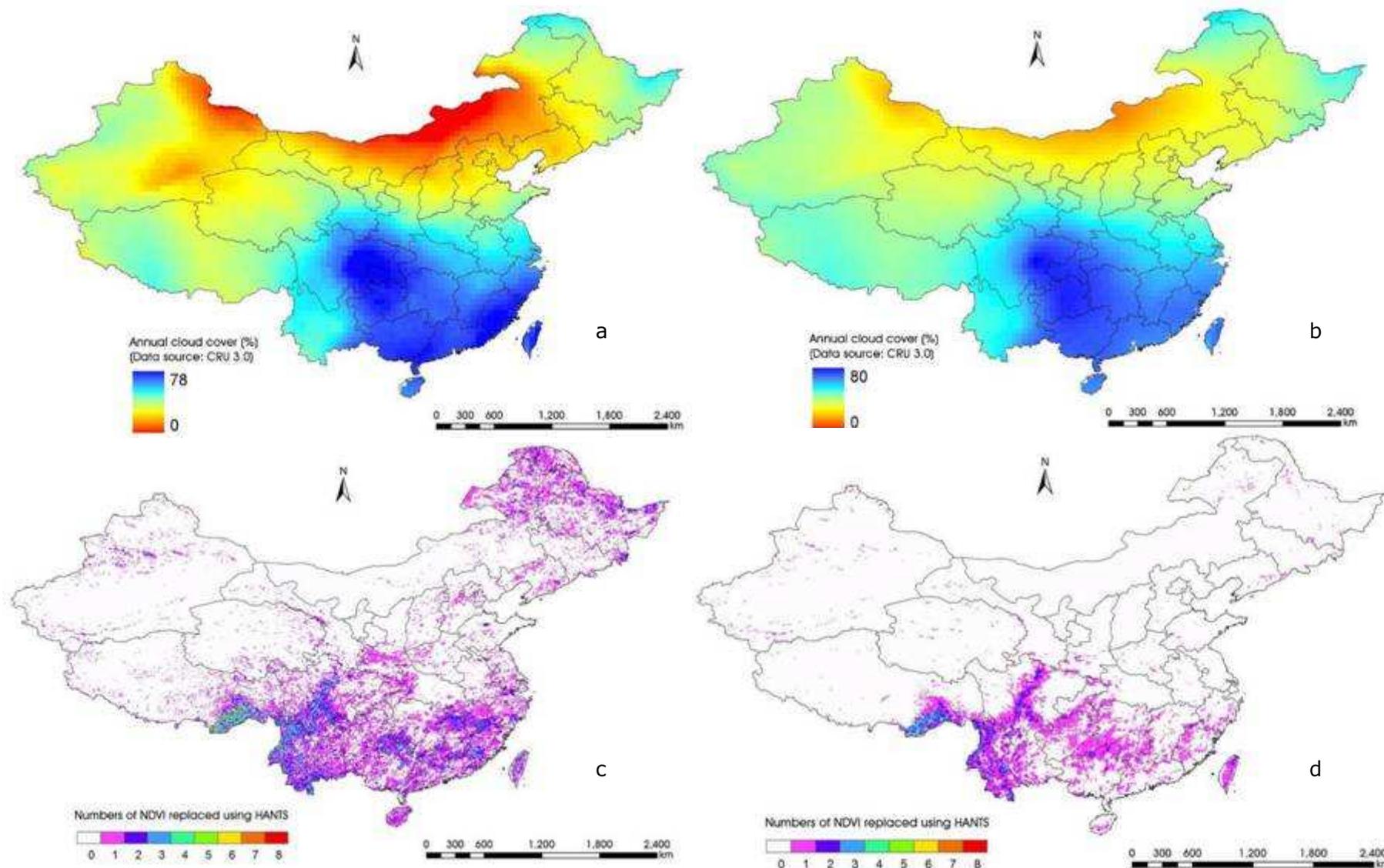
Figure A1. Annual mean cloud cover in 1998 (a), multi-year mean annual cloud cover 1981-2006 (b), numbers of GIMMS NDVI replaced using HANTS for year 1998 (c), and multi-year mean numbers of GIMMS NDVI replaced using HANTS for 1981-2006(d).